Reprinted from The Journal of Physical Chemistry, 1992, 96.

Thermodynamic Characterization of C_{60} by Differential Scanning Calorimetry†

Yimin Jin, Jinlong Cheng, Manika Varma-Nair, Guanghe Liang, Yigang Fu, Bernhard Wunderlich,*

Chemistry Division, Oak Ridge National Laboratory, Oak Ridge, Tennessee 37831-6197, and Department of Chemistry, The University of Tennessee, Knoxville, Tennessee 37996-1600

Xiao-Dong Xiang, Roman Mostovoy, and Alex K. Zettl

Materials Science Division, Lawrence Berkeley National Laboratory and Department of Physics, The University of California, Berkeley, California 94720 *(Received: December 23, 1991; In Final Form: February 18, 1992)*

Heat capacity measurements on C_{60} were carried out by differential scanning calorimetry from 120 to 560 K. This heat capacity was linked based on existing normal-mode and lattice calculation, to the vibrational heat capacities. In this way the thermodynamic functions are available from absolute zero of temperature. The phase transition at 256 K could be identified as a crystal-to-plastic crystal transition with an increase in entropy of 27.3 J/(K mol). A broad beginning of this transition at 190 K is linked to the change from a jumplike rotation that is starting already at about 100 K without increase in entropy to the rotational motion that ultimately causes the disordering transition. This classification is based on reinterpretation of the solid-state NMR results with calorimetry data. No melting temperature could be detected up to 950 K, the temperature limit of our calorimeter.

I. Introduction

Besides diamond and graphite, the two well-known crystalline allotropes of carbon, a totally new form of crystalline carbon has been discovered a few years ago.[1] It consists of ball-shaped C_{60} molecules (buckminsterfullerene) and has become well-known because of its special structure.[2] Before 1990 most research on C_{60} was limited to theoretical studies[3-12] because of insufficient material to undertake large-scale experimental studies. In 1990, Krätschmer et al. first reported a method to synthesize C_{60} in macroscopic quantity.[13,14]

Since then, the study of this new class of compounds and their derivatives is receiving more attention.[15,16] For example, there has been a characterization of the molecular structure using mass spectroscopy[1,2,4-8,13,14] and X-ray diffraction[14] as well as UV–vis light,[7,13,17,18] IR,[13,14,17-19] Raman,[20] NMR,[17,18,21-23] and ESR[17] spectroscopies and high-pressure liquid chromatography (HPLC).[17]

Initial information about a phase transition below room temperature became available recently through differential thermal analysis.[24-26] Coupled with X-ray data, orientational ordering was suggested to occur on cooling. In this paper measurements and computations of heat capacity will be reported. The computations are based on vibrational spectra. These new data permit a quantitative interpretation of the transition and, in addition, allow the generation of complete thermodynamic functions, of enthalpy (H), entropy (S), and Gibbs function (G).

The heat capacity of C_{60} was measured from 120 to 560 K by using a single-run differential scanning calorimetry (DSC) technique[27-29] which needs only 20–30-mg samples to produce quality data. The heat capacity contribution from vibrations was calculated next, based on existing normal-mode and lattice vibration frequencies,[9-12,30,31] and then compared with the experimental data. It will be shown that the phase transition that occurs at 256 K is a crystal-to-plastic crystal transition with an entropy of 27.3 J/(K mol), typical for such transitions involving orientational disordering. A broad beginning of this transition can be

† Presented at the American Physical Society Meeting, March 16–20, 1992.

linked to the change in motion from jumplike rotation, initiated already in the crystal at much lower temperature, to isotropic rotation. This interpretation is based on the known solid-state NMR spectrum[32-34] and confirmed, in this paper, by heat capacity investigations.

Finally, an effort to establish the melting temperature was limited to the observation that no melting occurred up to 950 K, the upper range of our DSC.

II. Experimental Section

Sample. Fullerenes were extracted from fullerene-rich soot (Texas Fullerenes, Inc.) using a Soxhlet extractor with benzene or hexane. The extracted C_{60} was separated from C_{70} and the higher fullerenes using an alumina chromatographic column. The C_{60} powder was then washed with ether and dried in vacuum at about 475 K. The purity of the sample was better than 99.5%, checked by mass and Raman spectroscopies.

Calorimetry. A commercial Thermal Analyst 2100 system from TA Instruments Inc. with a 912 dual-sample DSC and DSC autosampler were used for heat capacity measurements. Details about the equipment, operation, and software development were given in previous publications.[27-29] A single-run heat capacity measurement technique was used.[35] Heat capacities were determined from 120 to 560 K with four sets of experiments (120–220, 180–320, 310–420, and 380–500 K). Each run was repeated five times, and the collected data were averaged and smoothed. The error is estimated to be <1% above 300 K, <3% below 200 K, and <2% between 200 and 300 K.

All heat capacities were measured at 10 K/min heating rate with N_2 gas flow of 10 mL/min above 300 K and with stationary N_2 gas below 300 K. Heat capacities were calibrated with a sapphire standard. The temperature calibration was carried out using the onsets of the transition peaks for cycloheptane (134.8 and 265.1 K), 1-chlorobutane (150.1 K), cyclohexane (186.1 and 279.7 K), naphthalene (353.42 K), benzoic acid (396.55 K), indium (429.75 K), tin (505.05 K), and potassium nitrate (607.15 K). Sample masses were 20–30 mg. All sample placement was done with the autosampler for increased repeatability. No weight loss was observed over the temperature range of heat capacity analysis.

The preliminary check for a melting temperature was carried out at 50 K/min heating rate in a qualitative mode. The sample was enclosed for this experiment in a nonhermetically sealed copper pan. No melting temperature could be detected up to 950 K, the temperature limit of our calorimeter. The weight loss after this experiment, presumably through sublimation, was less than 2%.

Calculation of the Heat Capacity. The calculation of heat capacity of solids from vibrational spectra is well documented in several publications from our laboratory.[36-39] The heat capacity at constant volume (C_v) is calculated based on a separation of the vibrational spectrum into group and molecular vibrations. A molecule of C_{60} has a total of $N = 3 \times 60 = 180$ vibrational modes which consist of six molecular vibrations and 174 group vibrations. For each of the group vibrations one can use an Einstein function, $E(\theta_i)$

$$C_v = R\sum_{i=1}^{N} E(\theta_i) = R\sum_{i=1}^{N} \frac{(\theta_i/T)^2 e^{\theta_i/T}}{(e^{\theta_i/T} - 1)^2} \quad (1)$$

where N is number of vibrational modes, R is the gas constant, 8.314 54 J/(K mol), T is the temperature in K, and $\theta_i = h\nu_i/k$ is the characteristic frequency expressed in K. (A frequency, ν_i, given, as customary in spectroscopy, in wavenumbers, cm^{-1}, must be multiplied by 1.4388 cm K to yield frequency in K.)

The molecular vibrations form a more continuous spectrum, so that we divided the frequency distribution curves obtained from molecular dynamic simulations[30] at 100 K into a sufficiently closely spaced set of discrete frequencies to calculate the heat capacity contribution. A digitizer was used to convert the frequency distribution curves published in ref 30 (Figure 2) to a data file of θ vs $\rho(\theta)$, where θ and $\rho(\theta)$ are the frequency and its population, respectively. Then, their heat capacity contribution can be calculated by

$$C_{v,\text{molecular}} = 3R\frac{\int_0^\infty \rho_1(\theta)\, E(\theta)\, d\theta}{\int_0^\infty \rho_1(\theta)\, d\theta} + 3R\frac{\int_0^\infty \rho_2(\theta)\, E(\theta)\, d\theta}{\int_0^\infty \rho_2(\theta)\, d\theta} \quad (2)$$

where the sums are taken over the whole range of the distribution curves, including both translational (ρ_1) and librational (ρ_2) parts of the spectrum. A total of 6000 equally spaced frequencies were taken for the numeral integration that ranged from 0 to 60 cm^{-1} (acoustic vibrations).

All three sets of molecular normal-mode frequencies (group vibrations) reported in the literature[9,11,12] were used to calculate the heat capacity contributions

$$C_{v,\text{normal}} = \sum_{i=1}^{174} E(\theta_i) = \sum_{j=1}^{46} g_j E(\theta_j) \quad (3)$$

where $E(\theta_i)$ is the Einstein function and g_j is the degeneracy of vibration j ($\sum g_j = 174$). The frequencies are summarized in Table I.

The heat capacity at constant volume is then the sum of the two contributions (eqs 2 and 3):

$$C_v = C_{v,\text{molecular}} + C_{v,\text{normal}} \quad (4)$$

The conversion of heat capacity at constant volume to that at constant pressure, C_p, is done by a modified Nernst–Lindemann equation[40]

$$C_p - C_v = 3RA_0C_pT/T_m^\circ \quad (5)$$

where R is the gas constant, A_0 is a constant, either fitted to experimental data on compressibility and expansivity or approximated by the universal value of 3.9×10^{-3} (K mol)/J, and T_m° represents the equilibrium melting temperature. For C_{60}, the universal value of A_0 needed to be used because no compressibility and expansivity data are available. Finally, T_m° was estimated to be 1000 K.

Once the heat capacity is established, the enthalpy (H), entropy (S), and Gibbs function (G) can be easily calculated as follows

$$H = H^0 + \int_0^{T_d} C_p(T)\, dT + \Delta H_d + \int_{T_d}^{T} C_p(T)\, dT \quad (6)$$

$$S = \int_0^{T_d} \frac{C_p(T)}{T}\, dT + \Delta S_d + \int_{T_d}^{T} \frac{C_p(T)}{T}\, dT \quad (7)$$

$$G = H - TS \quad (8)$$

where ΔH_d and ΔS_d are the enthalpy and entropy of disordering at the equilibrium transition temperature T_d, and H^0 is the enthalpy and Gibbs function at absolute zero. The crystal at absolute zero is assumed to be sufficiently perfect to use the third-law entropy of zero.

III. Results

Heat Capacity of C_{60}. Experimental and calculated heat capacities of C_{60} are shown in Figure 1 for the temperature range 0–1000 K. The numerical data are listed in Table II from 120 to 560 K together with the differences between the experimental and calculated data.

Transitions. The order–disorder transition was detected at a heating rate of 10 K/min. The transition has a rather broad beginning at about 190 K. The equilibrium transition temperature was thus obtained by extrapolation of the steep low-temperature side of the transition peak to the heat capacity baseline at 256 K. This standard procedure in thermal analysis eliminates all instrument lag and is based on the assumption that the main part of the transition is a sharp first-order type.[41] The vibrational heat capacity is reached again at about 280 K. The peak temperature is 259 K. For all future calculations 256 K is used as the equilibrium transition temperature. The integrated enthalpy of the transition is 9.7 J/g or 6.99 kJ/mol (baseline established by the vibrational heat capacity between 190 and 280 K). The entropy of the disorder transition becomes then 27.3 J/(K mol).

An attempt has been made to find the possible melting temperature of C_{60} by using DSC with a nonhermetically sealed copper

TABLE I: Normal-Mode Vibration Frequencies for C_{60}

no. (j)	symmetry	I_h group label	frequency (ν_j), cm^{-1} 1989[a]	1988[b]	1987[c]	expt[d]	degeneracy (g_j)
1	$1A_g$	A_g	1830	1667	1627.4	1469	1
2	$2A_g$		510	610	547.6	497	1
3	$1T_{1g}$	T_{1g}	1662	1410	1463.8		3
4	$2T_{1g}$		1045	865	810.9		3
5	$3T_{1g}$		513	627	566.8		3
6	$1T_{3g}$	T_{3g}	1900	1483	1665.1		3
7	$2T_{3g}$		951	919	926.6		3
8	$3T_{3g}$		724	784	726.4		3
9	$4T_{3g}$		615	591	525.2		3
10	$1G_g$	G_g	2006	1650	1765.4		4
11	$2G_g$		1813	1404	1590.0		4
12	$3G_g$		1327	1235	1173.5		4
13	$4G_g$		657	856	672.7		4
14	$5G_g$		593	579	530.2		4
15	$6G_g$		433	491	455.8		4
16	$1H_g$	H_g	2068	1722	1830.7		5
17	$2H_g$		1910	1596	1688.2		5
18	$3H_g$		1575	1407	1398.5		5
19	$4H_g$		1292	1261	1160.0		5
20	$5H_g$		828	924	779.8		5
21	$6H_g$		526	771	552.4		5
22	$7H_g$		413	447	427.9		5
23	$8H_g$		274	263	272.0	273	5
24	$1A_u$	A_u	1243	972	1084.3		1
25	$1T_{1u}$	T_{1u}	1868	1628	1655.3		3
26	$2T_{1u}$		1462	1353	1374.1		3
27	$3T_{1u}$		618	719	550.9		3
28	$4T_{1u}$		478	577	491.3		3
29	$1T_{3u}$	T_{3u}	1954	1687	1720.1		3
30	$2T_{3u}$		1543	1314	1309.4		3
31	$3T_{3u}$		1122	1134	1019.0		3
32	$4T_{3u}$		526	776	626.6		3
33	$5T_{3u}$		358	348	361.8		3
34	$1G_u$	G_u	204	1587	1764.4		4
35	$2G_u$		1845	1436	1620.4		4
36	$3G_u$		1086	1110	958.3		4
37	$4G_u$		876	914	755.8		4
38	$5G_u$		663	750	701.9		4
39	$6G_u$		360	362	373.7		4
40	$1H_u$	H_u	2086	1709	1830.0		5
41	$2H_u$		1797	1467	1578.5		5
42	$3H_u$		1464	1344	1289.7		5
43	$4H_u$		849	822	770.3		5
44	$5H_u$		569	706	577.7		5
45	$6H_u$		470	546	491.6		5
46	$7H_u$		405	403	354.7		5
							174[e]

[a] Data from ref 12. [b] Data from ref 11. [c] Data from ref 9. [d] Data from ref 20. [e] Total number for the normal vibration modes of buckminsterfullerene.

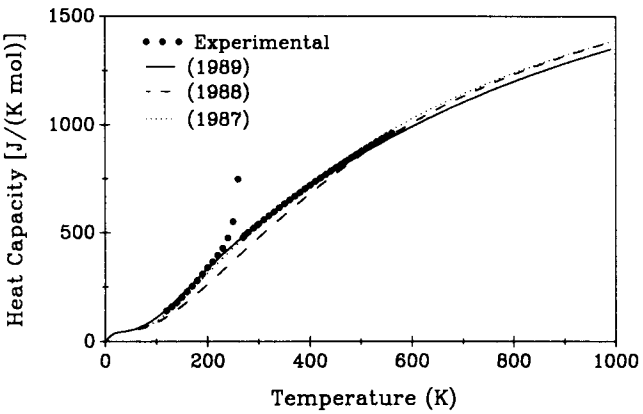

Figure 1. Calculated (lines) and experimental (symbol) heat capacities for C_{60}.

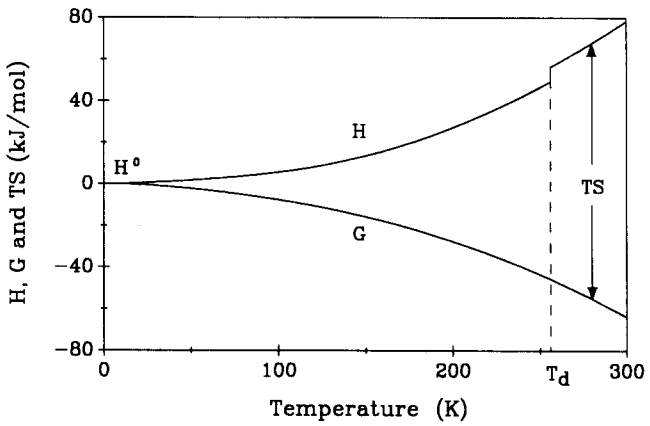

Figure 2. Thermodynamic functions for C_{60}. Note that $H - G = TS$. The amplitude is shifted by H^0, the enthalpy of C_{60} at absolute zero, to be zero.

pan. At a heating rate of 50 K/min, the sample did not show a significant transition up to 950 K where the instrument limit was reached. After heating, the weight loss of the sample was less than 2%.

Thermodynamic Functions. Thermodynamic functions H, S, and G have been established based on eqs 6–8 and are shown in Figure 2. Tabular values can be obtained from the authors on

TABLE II: Calculated and Experimental Heat Capacity of C_{60}

	heat capacity, J/(K mol)				deviation, %		
	calcd			expt			
T, K	1989[a]	1988[b]	1987[c]	(this work)	1989[a]	1988[b]	1987[c]
120	147.6	112.2	126.9	139.6	5.4	−24.4	−10
130	169.1	127.7	147.1	159.4	5.8	−24.8	−8.4
140	191.7	144.5	168.7	178.4	7.0	−23.4	−5.7
150	214.9	162.3	191.4	202.5	5.8	−24.8	−5.8
160	238.5	181.9	214.8	228.4	4.2	−26.3	−6.4
170	262.2	200.3	238.6	254.0	3.2	−26.8	−6.4
180	285.9	220.3	262.6	279.2	2.4	−26.7	−6.3
190	309.4	240.7	286.8	310.0	−0.2	−28.8	−8.1
200	332.6	261.6	310.9	338.3	−1.7	−29.3	−8.8
210	355.5	282.7	334.8	365.2	−2.7	−29.2	−9.1
220	378.0	304.1	358.5	395.5	−4.7	−30.1	−10.3
230	399.9	325.6	381.8	428.6	−7.2	−31.6	−12.2
240	421.4	347.2	404.9	475.5	−12.8	−37.0	−17.4
250	442.5	368.9	427.6	551.7	−24.7	−49.6	−29.0
260	463.2	390.6	450.0	748.6	−61.6	−91.6	−66.4
270	483.4	412.3	472.0	478.5	1.0	−16.1	−1.4
273.15	489.6	419.1	478.8	487.5	0.4	−16.3	−1.8
280	503.2	433.9	493.6	501.2	0.4	−15.5	−1.5
290	522.6	455.5	514.9	521.0	0.3	−14.4	−1.2
298.15	538.1	473.0	532.0	536.9	0.2	−13.5	−0.9
300	541.6	477.0	535.9	540.5	0.2	−13.3	−0.9
310	560.2	498.3	556.5	559.7	0.1	−12.3	−0.6
320	578.5	519.5	576.8	578.7	−0.0	−11.4	−0.3
330	596.5	540.5	596.8	597.3	−0.1	−10.5	−0.1
340	614.2	561.4	616.4	615.8	−0.2	−9.7	0.1
350	631.6	582.0	635.8	633.9	−0.4	−8.9	0.3
360	648.7	602.5	654.8	651.8	−0.5	−8.2	0.5
370	665.5	622.7	673.6	669.4	−0.6	−7.5	0.6
380	682.1	642.7	692.0	686.8	−0.7	−6.9	0.8
390	698.4	662.4	710.2	703.9	−0.8	−6.3	0.9
400	714.5	681.8	728.0	720.8	−0.9	−5.7	1.0
410	730.4	701.0	745.6	737.4	−1.0	−5.2	1.1
420	746.0	719.9	763.0	753.9	−1.0	−4.7	1.2
430	761.5	738.6	780.0	770.1	−1.1	−4.3	1.3
440	776.7	756.9	796.7	786.0	−1.2	−3.8	1.4
450	791.7	774.9	813.2	801.8	−1.3	−3.5	1.4
460	806.5	792.7	829.4	817.3	−1.3	−3.1	1.5
470	821.1	810.1	845.3	832.6	−1.4	−2.8	1.5
480	835.4	827.2	861.0	847.7	−1.5	−2.5	1.5
490	849.6	844.1	876.4	862.6	−1.5	−2.2	1.6
500	863.6	860.6	891.6	877.4	−1.6	−2.0	1.6
510	877.4	876.8	906.4	891.9	−1.6	−1.7	1.6
520	891.0	892.7	921.0	906.2	−1.7	−1.5	1.6
530	904.4	908.4	935.4	920.4	−1.8	−1.3	1.6
540	917.6	923.7	949.5	934.3	−1.8	−1.2	1.6
550	930.6	938.7	963.3	948.1	−1.9	−1.0	1.6
560	943.4	953.4	976.9	961.7	−1.9	−0.9	1.6
avg error (excluded transition between 220 and 260 K)					0.09	−11.49	−1.33
rms error (excluded transition between 220 and 260 K)					2.33	9.47	3.64

[a] Calculation based on the frequencies given by Weeks et al.[12] [b] Calculation based on the frequencies given by Satanton et al.[11] [c] Calculation based on the frequencies given by Wu et al.[9]

request through our ATHAS data bank.[42]

IV. Discussions

Heat Capacity. The measured heat capacity C_p of C_{60} agrees reasonably well with the calculated heat capacities based on the various vibrational frequencies, as shown in Figure 1. Since three sets of normal-mode calculations of the group vibrations were reported independently, we have combined each of these individually with the molecular vibrations to calculate the heat capacity. The differences among the group vibration spectra are obvious not only from the frequency table (Table I) but also from the deviations between calculated and measured heat capacities (Table II). The best agreement is obtained with the data by Weeks et al.[12] These authors reviewed also the two prior sets of calculations and concluded (in agreement with the present heat capacity measurements) that the gata given by them are computed by a better method and force field. The later published experimental (IR) frequencies[24] show also a somewhat better agreement with Weeks' results in the lower frequencies, critical for heat capacity computation (see Table II). As can be seen from Figure 1, further improvement of the normal-mode calculations can hardly be checked by C_p measurement.

Getting close to the limit of precision of the experimental C_p, one notices a small positive deviation of the computed C_p below 190 K. Although this may be caused by experimental error, it may also be an indication of the smaller heat capacity contribution of jumplike motion relative to vibration. Since three of the fully excited skeletal modes at this temperature could be involved in such change of motion, the maximum decrease in heat capacity would be $3/2R$ or 12.5 J/(K mol), or about 6% of the total C_p at about 150 K.

The increasingly negative deviation of the calculated heat capacity between 190 and at least 260 K is due to the orientational disorder which will be discussed in the next section.

Finally, the small negative deviation above 400 K might easily be caused by the increasing importance of the C_v to C_p conversion in which A_0 and $T_m°$ had to be estimated. At 150 K the C_p is larger than C_v by 1.5%, at 250 K by 2.6%, at 350 K by 3.7%, at 450 K by 4.8%, and at 550 by 6.0%. The experience in heat capacities of polymeric samples[44] has revealed a typical error of

about 50% for A_0; i.e., the resulting C_p is well within the shown deviations. Note that one expects C_v to be more precise than C_p.

It must be mentioned here that the heat capacity contribution from the lattice vibrations ($6R$) derived from the molecular dynamics simulation[30] is relatively small, compared to that from the group vibrations, and is almost constant in the region of experimental data, above 100 K [full excitation yields a contribution to $C_v \approx 50$ J/(K mol)]. To verify the precision of the heat capacities below 100 K, low-temperature experiments must be done. Since the heat capacity at low temperature is, however, small, one does not expect significant changes in the thermodynamic functions at high temperature.

Transition and Motions. An orientation disorder transition at about 260 K was reported earlier by several authors[24-26,32-34] and had been confirmed by DSC,[24-26] X-ray diffraction,[24] solid-state NMR,[32-34] and molecular dynamics simulation.[30] The reported transition parameters varied from 249 to 264 K for the transition temperature,[24,26] and from 6.7 to 9.2 J/g for the enthalpy of transition,[24,26] because of differences in purity and differences in defining the transition temperature and use of an empirical baseline for the separation of the transition peak. On the basis of our calculated, vibration-only heat capacity, we were able to establish the correct baseline for the transition. It reaches from 190 to 280 K, and the enthalpy of transition increases then to a value of 9.7 J/g, 45–5% above the prior reported data. The equilibrium transition temperature of 256 K was chosen since the transition peak temperature may change with sample mass.

With these new values a somewhat larger transition entropy of 27.3 J/(K mol) results. This value is typical for a crystal-to-plastic-crystal transition which normally has an orientational disordering transition entropy ranging from 20 to 50 J/(K mol).[41] This value also reconfirms the observation that the entropy of orientational disordering is independent of molecular size.[43] Directly measured entropies of disordering of carbon tetrachloride, 2,3-dimethylbutane, cyclohexanol, camphor, and C_{60} range only between 20 and 47 J/(K mol).[44] It has been confirmed by X-ray diffraction and solid-state NMR that the crystal of C_{60} at room temperature is completely orientationally disordered and has a fcc cubic crystal structure, typical for plastic crystals.

Several research groups[32-34] have reported that, in the solid-state ^{13}C NMR spectrum of a static sample, a sharp peak emerges at about 100 K from the broad resonance of the chemical shift anisotropy powder pattern. This suggests that orientational motion in C_{60} starts already at such low temperatures. The observed motion below 190 K does, however, not cause any entropy of orientational disordering, as is shown by the heat capacities of Table II. Thus, the motion must consist of jumps between symmetry-equivalent orientations, presumably in 72° (5-fold) steps. This interpretation is based on the combined results of thermal analysis *and* simple NMR experiments and is consistent with the general conclusions made by Tycko et al.[34] through their study of the temperature dependence of the ^{13}C spin–lattice relaxation time (T_1). A break at about the same temperature, ca. 190 K, is apparent in their plot of T_1 (Figure 1 of ref 34) but was not discussed at that time. Coupled with calorimetry it gains importance as upper temperature limit of pure jump motion without entropy increase. Above 190 K, the heat capacity shows increasing entropic contributions, indicating beginning orientational disorder.

The time scale of the orientational motion in C_{60} was also evaluated by NMR studies and can now be more clearly interpreted. Solid-state ^{13}C NMR results indicate that at about 100 K the orientational jumps have a correlation time of 50 μs, as estimated from the inverse of the spectral spread of the chemical shift anisotropy power pattern.[32,33]

With increasing temperature, the jump motion becomes faster and the correlation time, τ, follows above 190 K a proposed Arrhenius law (obtained from a fit to the temperature-dependent ^{13}C T_1 data from 190 to about 240 K)[34]

$$\tau = 3.12 \times 10^{-14} \exp(24100/RT) \qquad (9)$$

with time in seconds and R in J/(K mol).

Assuming that τ for this jumplike motion with increasing orientational disorder has a typical value of 5 ns at the crystal-to-plastic crystal transition, an average value for a large number of close to spherically symmetric molecules that was documented by Boden,[45] the equation above predicts a disordering temperature of 243 K, in good agreement with that reported in this paper (256 K). Above $T_d = 256$ K, the variously reported correlation times are all within the range of that for plastic organic solids ($\tau = 5$ ns at T_d, decreasing to 2 ps at isotropization[45]).

In summary, there are three temperature regions of different types of rotational motions in C_{60}. The rotational oscillations described by the molecular vibrations of eq 2 change, starting at about 100 K, to allow occasional jumps to symmetry-related orientations. The second type of rotational motion involves a typical pretransitional motion described by eq 9 starting already at 190 K and involves in addition to the motion at lower temperature rotational disorder. Above 256 K a phase change with crystal structure change has taken place, and the rotational motion is that typical for a plastic crystal. On ultimate isotropimerization, above 950 K, no more than an additional 7–14 J/(K mol) is expected for the positional disordering.

Thermodynamic Functions of C_{60}. By knowing the heat capacity of C_{60}, thermodynamic functions of C_{60} can be easily calculated based on eqs 6–8. The data have been plotted in Figure 2. As mentioned above, tabular values are available through the ATHAS data bank.[42] With the knowledge of heat capacity the data shown can easily extrapolated to 1000 K and above. The final discontinuity in enthalpy on isotropization should have an approximate value of 10 kJ ($\approx$1000 K × 10 J/K), about the same order of magnitude as the disordering at 256 K. It is surprising to see such a large temperature range of stability of the plastic crystalline C_{60}. One may even speculate that the beginning of the translational diffusive motion may be gradual and not lead to a sharp transition. Sublimation and high temperature complicate research of this topic. We hope to find more details in the future.

Acknowledgment. This work was supported by the Division of Materials Research, National Science Foundation, Polymers Program, Grant DMR 8818412, and the Division of Materials Sciences, Office of Basic Energy Sciences, U.S. Department of Energy, under Contract DE-AC05-84OR21400 with Martin Marietta Energy Systems, Inc. The work at University of California, Berkeley, involved mainly the sample preparation and is supported by DOE under Contract DE-AC03-76SF00098.

Registry No. C_{60}, 99685-96-8.

References and Notes

(1) Rohlfing, E. A.; Cox, D. M.; Kaldor, A. J. *J. Chem. Phys.* **1984**, *81*, 3322.
(2) Kroto, H. W.; Heath, J. R.; O'Brien, S. C.; Curl, R. F.; Smalley, R. E. *Nature* **1985**, *318*, 162.
(3) Marks, R. W. *The Dymaxion World of Buckminster Fuller*; Reinhold: New York, 1960. Fuller, R. B. *Ideas and Integrities*; Collier Books: New York, 1963.
(4) Zhang, Q. L.; O'Brien, S. C.; Heath, J. R.; Liu, Y.; Curl, R. F.; Kroto, H. W.; Smalley, R. E. *J. Phys. Chem.* **1986**, *90*, 525.
(5) Liu, Y.; O'Brien, S. C.; Zhang, Q.; Heath, J. R.; Tittel, R. K.; Curl, R. F.; Kroto, H. W.; Smalley, R. E. *Chem. Phys. Lett.* **1986**, *126*, 215.
(6) Elser, V.; Haddon, R. C. *Nature* **1987**, *325*, 792.
(7) Curl, R. F.; Smalley, R. E. *Science* **1988**, *242*, 1017.
(8) Kroto, H. *Science* **1988**, *242*, 1139.
(9) Wu, Z. C.; Jelski, D. A.; George, T. F. *Chem. Phys. Lett.* **1987**, *137*, 291.
(10) Weeks, D. E.; Harter, W. G. *Chem. Phys.* **1988**, *144*, 366.
(11) Stanton, R. E.; Newton, M. D. *J. Phys. Chem.* **1988**, *92*, 2141.
(12) Weeks, D. E.; Harter, W. G. *J. Chem. Phys.* **1989**, *90*, 4744.
(13) Krätschmer, W.; Fostiropoulos, K.; Huffman, R. *Chem. Phys. Lett.* **1990**, *170*, 167.
(14) Krätschmer, W.; Lamb, L. D.; Fostiropoulos, K.; Huffman, D. R. *Nature* **1990**, *347*, 354.
(15) Baum, R. *Chem. Eng. News* 1991 (July), 4.
(16) Smalley, R. E. In *Atomic and Molecular Clusters*; Bernstein, E. R., Ed.; Elsevier: New York, 1990.
(17) Cox, D. M.; Behal, S.; Disko, M.; Gorun, S. M.; Greaney, M.; Hsu, C. S.; Kollin, E. B.; Millar, J.; Robbins, J.; Robbins, W.; Sherwood, R. D.; Tindall, P. *J. Am. Chem. Soc.* **1991**, *113*, 2940.
(18) Ajie, H.; Alvarez, M. M.; Anz, S. J.; Beck, R. D.; Diederich, F.; Fostiropoulos, K.; Huffman, D. R.; Krätschmer, W.; Rubin, Y.; Schriver, K.

E.; Sensharma, D.; Whetten, R. L. *J. Phys. Chem.* **1990**, *94*, 8630.
(19) Haufler, R. E.; Conceicao, J.; Chibante, J. P. F.; Chai, Y.; Byrne, N. E.; Flanagan, S.; Haley, M. M.; O'Brien, S. C.; Pan, C.; Xiao, Z.; Billups, W. E.; Ciufolini, M. A.; Hauge, R. H.; Margrave, J. L.; Wilson, L. J.; Curl, R. F.; Smalley, R. E. *J. Phys. Chem.* **1990**, *94*, 8634.
(20) Bethune, D. S.; Meijer, G.; Tong, W. C.; Rosen, H. J. *Chem. Phys. Lett.* **1990**, *174*, 219.
(21) Taylor, R.; Hare, J. P.; Abdul-Dada, A. K.; Kroto, H. W. *J. Chem. Soc., Chem. Commun.* **1990**, 1423.
(22) Johnson, R. D.; Meijer, G.; Bethune, D. S. *J. Am. Chem. Soc.* **1990**, *112*, 8983.
(23) Johnson, R. D.; Meijer, G.; Salem, J. R.; Bethune, D. S. *J. Am. Chem. Soc.* **1991**, *113*, 3619.
(24) Heiney, P. A.; Fischer, J. E.; McGhie, A. R.; Romanow, W. J.; Denenstein, A. M.; McCauley Jr., J. P.; Smith III, A. B. *Phys. Rev. Lett.* **1991**, *66*, 2911.
(25) McGhie, A. R.; Romanmow, W. J.; Denenstein, A.; Fischer, J. E.; Heiney, P. A.; Selig, H.; Coustel, N.; Allen, B.; McCauley Jr., J. P.; Smith III, A. B. In *Proceedings of the 20th NATAS Conference*; Keating, M. Y., Ed.; Minneapolis, MN, Sept 1991; p 405.
(26) Siemens, R. L.; Johnson, R. D.; Dorn, H. C.; Bethune, D. S.; Brown, C. A.; Lyerla, J.; Yannoni, C. S.; Wendt, H. R.; de Vries, M.; Taylor, L.; Jedrzejewski, P.; Salem, J. R. In *Proceedings of the 20th NATAS Conference*; Keating, M. Y., Ed.; Minneapolis, MN, Sept 1991; p 559.
(27) Jin, Y.; Wunderlich, B. *J. Therm. Anal.* **1990**, *36*, 765.
(28) Jin, Y.; Wunderlich, B. *J. Therm. Anal.* **1990**, *36*, 1519.
(29) Jin, Y.; Wunderlich, B. *J. Therm. Anal.*, in press.
(30) Cheng, A.; Klein, M. L. *J. Phys. Chem.* **1991**, *95*, 6750.
(31) Raghavachari, K.; Rohlfing, C. M. *J. Phys. Chem.* **1991**, *95*, 5768.
(32) Yannoni, C. S.; Johnson, R. D.; Meijer, G.; Bethune, D. S.; Salem, J. R. *J. Phys. Chem.* **1991**, *95*, 9.
(33) Tycko, R.; Haddon, R. C.; Dabbagh, G.; Glarum, S. H.; Douglass, D. C.; Mujsce, A. M. *J. Phys. Chem.* **1991**, *95*, 518.
(34) Tycko, R.; Dabbagh, G.; Fleming, R. M.; Haddon, R. C.; Makhija, A. V.; Zahurak, S. M. *Phys. Rev. Lett.* **1991**, *67*, 1886.
(35) Wunderlich, B. *J. Therm. Anal.* **1987**, *32*, 1949.
(36) Cheban, Yu. V.; Lau, S. F.; Wunderlich, B. *Colloid Polym. Sci.* **1982**, *260*, 9.
(37) Lau, S.-F.; Wunderlich, B. *J. Therm. Anal.* **1983**, *28*, 59.
(38) Loufakis, K.; Wunderlich, B. *J. Phys. Chem.* **1988**, *92*, 4205.
(39) Bu, H. S.; Cheng, S. Z. D.; Wunderlich, B. *J. Phys. Chem.* **1987**, *91*, 4179.
(40) Pan, R.; Varma-Nair, M.; Wunderlich, B. *J. Therm. Anal.* **1989**, *35*, 955.
(41) Wunderlich, B. *Thermal Analysis*; Academic Press: Boston, 1990.
(42) ATHAS data bank update, 1991; Dr. B. Wunderlich, Department of Chemistry, University of Tennessee, Knoxville, TN 37996-1600.
(43) Wunderlich, B. *Macromolecular Physics*; Academic: New York, 1980; Vol. 3.
(44) Wunderlich, B.; Möller, M.; Grebowicz, J. *Adv. Polym. Sci.* **1984**, *60/61*, 1.
(45) Boden, N. NMR Studies of Plastic Crystal. In *The Plastically Crystalline State (Orientationally-Disordered Crystals)*; Sherwood, J. N., Ed.; John Wiley and Sons: Chichester, 1979.